NMR comparative study of $PbMg_{1/3}Nb_{2/3}O_3$ and $PbSc_{1/2}Nb_{1/2}O_3$ local structure.

V. V. Laguta, M. D. Glinchuk, S. N. Nokhrin, and I. P. Bykov,
Institute for Problem of Material Sciences, Ukrainian Academy of Sciences,
Krjijanovskogo 3, 03142 Kiev, Ukraine

R. Blinc, A. Gregorovič, and B. Zalar
Jožef Stefan Institute, P. O. Box 3000, 1001 Ljubljana, Slovenia
(February 1, 2008)

Abstract

The ^{93}Nb and ^{45}Sc NMR spectra in $PbSc_{1/2}Nb_{1/2}O_3$ (PSN) and $PbMg_{1/3}Nb_{2/3}O_3$ (PMN) disordered relaxor ferroelectrics at the temperature $T > T_0$ (T_0 is the temperature of the dielectric susceptibility maximum) have been studied. Spectra analysis was performed on the base both of the analytical description of NMR lines shapes, allowing for homogeneous and inhomogeneous broadening related to a random distribution of the electric field gradients and numerical Monte Carlo method taking into account electric field gradients originated from random distribution of Mg, Sc and Nb ions (which may be shifted or not) over B-type cation sites.

The observed 1/2 $\longleftrightarrow$ -1/2 transition spectrum both of the ^{93}Nb and ^{45}Sc nuclei in the PSN was shown to contain a narrow (3-4 kHz) almost isotropic part and a broad strongly anisotropic part. These two components of NMR spectra are related to 1:1 Sc/Nb ordered and compositionally disordered regions of the crystal, respectively. It was shown that in the disordered regions Sc^{3+}, $Nb^{5+}$and O^{2-} ions are shifted from their cubic lattice sites at one of three possible directions: $< 100 >$, $< 110 >$ or $< 111 >$.

In PMN the NMR spectrum of ^{93}Nb contains practically only the broad component. The portion of unbroadened spectrum that may correspond to ideal 1:2 regions accounts only for 1-2 percent of the total integral intensity. No evidance was obtained about existence of the 1:1 regions in PMN. The NMR data demonstrate that in PMN the cubic symmetry at $T > T_0$ is locally broken due to ions shifts similar to that in disordered PSN. The values of the ion shifts were estimated in the point charges point dipoles approximation of the electric field gradients calculation both in the PSN and PMN.

77.84.Dy, 76.30.Fc

.

I. INTRODUCTION

Relaxor ferroelectrics [1,2] have been attracting considerable attention in recent years due to their unusual physical behavior. Lead magnesium niobate, $PbMg_{1/3}Nb_{2/3}O_3$ (PMN), is probably the best investigated perovskite relaxor crystal. Many of novel models which try to describe the physical properties of PMN are grounded on the assumption of the existence of a 1:1 Mg/Nb ordered microregions at least in 1/3 of the volume of a crystal. On the other hand, the latest x-ray and neutron diffraction measurements performed on the $PbSc_{1/2}Nb_{1/2}O_3$ (PSN) with different degree of cation ordering show that ferroelectric phase transition undergoes in both ordered (1:1 Sc/Nb) and completely disordered samples [3]. It might mean that long-range ordering can not be suppressed completely by compositional (chemical) disorder. Moreover, a large shifts of all type of ions from cubic regular positions in PMN as well as in PSN already at $T > T_0$ (T_0 represents the temperature of dielectric constant maximum) were obtained from the computer treatment of the x-ray and neutron diffraction peaks. Due to this, the phase transition even in PSN becomes incomprehensible because, as it follows from x-ray data, at $T > T_0$, for instance, Pb^{2+} ions are shifted away of about 0.027 nm with equal probability along one of the directions $< 100 >$, $< 110 >$ or $< 111 >$. This consideration left unclear, however, if these ion shifts are the static or dynamical ones.

Another difficulty in the interpretation of the x-ray and neutron diffraction data in relaxors is related to amorphous character of observed diffraction peaks even at $T << T_0$. These methods provide an averaged view of the structure resulting in the cubic (PMN) or close to cubic symmetry (PSN). Broadening of diffraction peaks is caused by the compositional disorder of these materials. Thus, local methods of magnetic resonance and, in particular, Nuclear Magnetic Resonance (NMR) can be extremely useful in the study of such disordered systems because in NMR experiment the nuclei are sensitive to their environment only at a distance less then 1 - 2 nm. It provides also possibility to distinguish between the static and dynamic ion shifts that is practically unattainable in x-ray diffraction methods.

In our previous papers (see, for instance, Ref. [4]) we have already studied ^{93}Nb and ^{45}Sc NMR spectra both in the PMN and PSN. In particular, it was shown that at $T >> T_0$ NMR spectra of ^{93}Nb are mainly determined by the electric-field-gradient contribution originated from disorder in Nb/Mg(Sc) lattice sites. From NMR spectra analysis evidences were obtained about the existence of ordered and disordered microregions in both materials. Unfortunately, earlier measurements were carried out mainly at a low Larmor frequency ($\nu_L \simeq 49$ MHz) so a bigger part of the ^{93}Nb spectrum belonging even to $1/2 \longleftrightarrow -1/2$ transition remained invisible and could not be analysed. More detailed ^{93}Nb and ^{45}Sc NMR spectra were recently presented in Ref. [5] and [6]. However, only the temperature dependence of the second moment of the narrow subset of NMR lines has been analysed. A broad background observed in the spectrum was attributed to unresolved satellite transitions and it was not analysed.

The purpose of the present paper is to study local structure both of PMN and PSN at temperatures $T > T_0$ on the base of ^{93}Nb and ^{45}Sc NMR measurements performed at Larmor frequency $\nu_L \simeq 93$ MHz. We believe that complete $1/2 \longleftrightarrow -1/2$ transition spectrum can

be observed in such conditions. Because one of studied materials (PSN) belongs to a 1:1 system, where the 1:1 Sc/Nb order really exists it should be thus interesting to see what are the common features and what are the differences in NMR spectra of these two types of relaxors.

Description of the NMR line shape was performed on the base of analytical formulas, allowing for both homogenious and inhomogenious mechanisms of line broadening. As a second method of NMR spectra analysis we used numerical Monte Carlo simulation, which allowed to take into account random distribution of Mg, Nb and Sc ions (shifted away or not) over B-type sites of $AB'B''O_3$ perovskite lattice.

The structural data obtained are compared with analogous data resulting from x-ray diffraction methods. Finally, the problem of 1:1 Mg/Nb ordered microregions in PMN is discussed as well.

II. SAMPLES AND EXPERIMENTAL DETAILS

The measurements were carried out on single-crystal samples of PMN and PSN grown on a seed crystal from solution in melt. Samples had a good optical quality. The sample dimensions of PSN were (4x4x4) mm^3, and PMN - up to (8x8x8) mm^3 with the surfaces parallel to crystallographic (001) planes.

The NMR measurements were performed in a 9.2 T superconducting magnet at ^{45}Sc Larmor frequency ν_L = 92.3 MHz (I = 7/2) and ^{93}Nb ν_L = 92.9 MHz (I = 9/2). Temperature was stabilized in a continuous-flow cryostat with an accuracy of about 0.1 K. The inhomogeneously broadened spectra of ^{93}Nb and ^{45}Sc (1/2 $\longleftrightarrow$ -1/2 transition) have been obtained using the Fourie transform of the spin echo after a 90_x - τ - 90_y - τ - acquisition pulse sequence. The width of the 90^0 pulse was 2.1 μs and 2.4 μs for ^{93}Nb and ^{45}Sc resonances, respectively. A time delay τ was usually 40 μs for both of nuclei.

III. EXPERIMENTAL RESULTS AND THEIR INTERPRETATION

A. ^{93}Nb and ^{45}Sc NMR spectra

Measurements were performed at T = 400 - 450 K because we were interested mainly in the local structure of PMN and PSN in high temperature phase, i. e., at $T > T_0$ ($T_0 \approx$ 355 K and 310 K for PSN and PMN, respectively). As an example in Fig. 1 we presented ^{45}Sc NMR spectra measured for three characteristic crystal orientations in the external magnetic field: B II [001], [011] and [111] . The characteristic feature of the spectrum for B II [001] and [111] is its strong asymmetry while for B II [011] the spectrum is almost symmetric. Similar spectra of ^{93}Nb in the PSN and PMN are shown in Figs. 2 and 3, respectively. Let us discuss first the Sc and Nb spectra in the PSN.

Both the Sc and Nb spectra have approximately similar structure and both contain a narrow component of the width of (3 - 4) kHz and a wide component that is different for the Sc and Nb nuclei. The narrow part of spectra is well described by a Gaussian and is completely isotropic. On the contrary, the wide part is essentially anisotropic and can not be precisely described by a simple function. In rough approximation, however, it can be also

described by a Gaussian (see in Ref. [6]). In such approach the ratio of integral intensity of narrow and wide parts of the spectrum is approximately equal (40:60) and does not depend on the crystal orientation. Note that due to large width of the ^{93}Nb spectrum its wide component has very small intensity and thus its anisotropy manifests itself much less than that in the ^{45}Sc spectrum. However measurement of whole the ^{93}Nb spectrum in PSN, using the sweep of the irradiation frequency, indeed showed that the Nb spectrum shape is very close to that for ^{45}Sc (insert to Fig. 2).

^{93}Nb spectrum in PMN is somewhat complicated. In this spectrum we can conditionally separate three components: (1) low-intensity isotropic line with the width of 3 kHz; (2) spectrum around ν_L with the width of 15 - 18 kHz; (3) wide and strong anisotropic component like that in PSN but more intensive. The narrow part with $\Delta\nu = 3$ kHz accounts only for about 1.5 - 2 percent of the total integral intensity of the spectrum. As can be seen from Fig. 3, beside the narrowest component the whole spectrum is strongly anisotropic.

The anisotropy of spectra as well as asymmetric form with respect to ν_L for both of ^{93}Nb and ^{45}Sc nuclei and in both the PMN and PSN points out that given spectra belong to $1/2 \longleftrightarrow$ -1/2 transition the frequency of which is shifted by the second order quadrupolar contributions [7]. This quadrupole contribution exists only for nuclei with spin I $> 1/2$ and is related to the interaction of the nuclear quadrupole moment with the electric field gradient (EFG). Large values of quadrupole moments of ^{93}Nb and ^{45}Sc niclei ($eQ = -0.28e \cdot 10^{-28}$ m^2 and $-0.22e \cdot 10^{-28}$ m^2 for ^{93}Nb and ^{45}Sc, respectively) usually result in predominance of the quadrupole contribution to NMR frequency shift with respect to other possible sources, as chemical shift and magnetic dipole-dipole interaction. Therefore we can draw conclusion that main features of ^{93}Nb and ^{45}Sc NMR spectra in both the PMN and PSN are related to characteristic features of their EFG, that depend on a lattice ions charges and their positions, i.e. local structure of crystals.

B. Analysis of ^{45}Sc and ^{93}Nb spectra in PSN

The integral intensity ratio (40:60) obtained above for the narrow and wide parts of the ^{45}Sc and ^{93}Nb NMR spectra in PSN is in agreement with the Sc/Nb degree of ordering which varied in the studed crystals in the range of 30 - 40 percent. So, it can be assumed that narrow and wide parts of the spectra belong to the Sc and Nb nuclei situated in the ordered 1:1 and disordered regions of the crystal, respectively. Actually, in the ordered regions Sc and Nb ions are surrounded by a symmetrical ion configuration. Therefore in such sites the electric-field-gradients and anisotropic chemical shift must be close to zero and we can expect a NMR line broadened only by the magnetic dipole-dipole interaction. Calculation of this dipole-dipole width gives the value of about 3 kHz supporting the origin (ordered 1:1 regions) of narrow lines in ^{45}Sc and ^{93}Nb NMR spectra.

Evidently, the wide part of NMR spectra belongs to resonances from nuclei located in the disordered regions of the crystal, where random distribution of nonequal charges B$'$/B$''$ ions produce electric-field-gradients. It follows from recent x-ray and neutron diffraction data [3] that in these regions the lead and oxygen ions may be shifted away from their regular cubic positions of about 0.01 to 0.035 nm, which gives an additional contribution to the EFG tensor components. Of course, due to disorder in the ions positions we can expect broad

distribution in values of the EFG tensor components which manifestes in inhomogeneous broadening of NMR lines.

The resonance frequency shift related to quadrupole mechanism for the considered case of $\pm$ 1/2 transition is proportional to the squared EFG. It can be written as follows

$$\nu_{1/2}^{(2)} = \frac{\nu_Q^2}{6\nu_L}\left(I\left(I+1\right) - \frac{3}{4}\right) f_\eta(\theta,\varphi), \tag{1}$$

where $\nu_Q = \frac{3e^2qQ}{2I(2I-1)h}, eq = V_{zz}, \eta = \frac{V_{xx}-V_{yy}}{V_{zz}}$.

The function $f_\eta(\theta,\varphi)$ in Eq.(1) describes the dependence of frequency shift on mutual orientations of external magnetic field and EFG tensor principal axes, ν_L is the Larmor frequency, x,y,z form the pricipal EFG tensor reference frame.

Angular variation of the wide part of NMR spectra can be qualitatively understood if to assume presence of an axial EFG pointed at <001> cubic directions. In this case angular part of expression (1) takes a simple form:

$$f(\theta,\varphi) = -\frac{3}{8}\left(1-\cos^2\theta\right)\left(9\cos^2\theta - 1\right). \tag{2}$$

Expected resonances for all six <001> directions of the EFG tensor are depicted as hystograms in Fig. 1. In this our simple interpretation we have to take into account that due to large disorder in the ions positions EFG values become randomly distributed that leads to strong inhomogeneous broadening of NMR lines. As a result, only the shift of the center of gravity is visible in the experimental spectrum under crystal rotation. Obviously, that because of nonlinear relation between resonance frequency shift and quadrupole frequancy inhomogeneously broadened NMR line acquires essentially asymmetrical form, which besides depends on orientation of a crystal in external magnetic field. For such complex spectrum its decomposition on simple Gaussian components and the analysis of their angular dependence can not give true values of quadrupole frequencies.

In what follows, we introduce the distribution of largest EFG component which leads to the distribution of quadrupole frequencies ν_Q. Let us suppose that this distribution function can be expressed in Gaussian form, i. e.

$$F(\nu_Q) = \frac{1}{\sqrt{2\pi}\Delta}\exp(-\frac{(\nu_Q-\nu_Q^0)^2}{2\Delta^2}), \tag{3}$$

where ν_Q^0 is the mean value of the quadrupole frequency and Δ is the width of its distribution.

Allowing for the nonlinear relation between ν and ν_Q (see Eq.(1)), namely

$$\nu = \alpha\nu_Q^2,\ \alpha \equiv \frac{1}{6\nu_L}\left(I\left(I+1\right) - \frac{3}{4}\right) f(\theta,\varphi), \tag{4}$$

the shape of inhomogeneously broadened line can be written as (Ref. [8])

$$P(\nu) = \sum_{j=1}^{2}\frac{F(\nu_Q=\nu_{Qj})}{\mid \frac{d\nu}{d\nu_Q}\mid_{\nu_Q=\nu_{Qj}}},\ \nu_{Q_{1,2}} = \pm\sqrt{\frac{\nu}{\alpha}}. \tag{5}$$

Substitution of Eq.(3) into Eq.(5) gives

$$P(\nu) = \frac{1}{\sqrt{2\pi\alpha\nu}\Delta} \exp(-\frac{\nu + \alpha(\nu_Q^0)^2}{2\alpha\Delta^2}) \cosh \frac{\alpha}{\Delta^2}\sqrt{\frac{\nu}{\alpha}}. \quad (6)$$

To take into account the additional homogeneous broadening mechanism with Gaussian lineshape (dipole-dipole interactions) one has to make the integration

$$I(\nu) = \frac{1}{\sqrt{2\pi}\delta} \int_{-\infty}^{\infty} P(\nu') \exp\left[\frac{-\ln 2(\nu - \nu')^2}{\delta^2}\right] d\nu', \quad (7)$$

where δ being a half of the Gaussian width.

One can see that Eqs. (6-7) give an asymmetrical lineshape which depends also on the parameter $\alpha(\theta, \varphi)$ that takes into account the mutual orientations of EFG and magnetic field B_0.

One can expect that in disordered materials there are microregions with different ″degree of order″ and different directions (and mean values) of the ion displacements. Obviously, in such a case the NMR line should be the composition of the lines ″stemming″ from these microregions, i.e.

$$I_q(\nu) = \sum_i I_{qi}(\nu) \quad (8)$$

where subscript ″i″ numerates the microregions.

The results of simulation on the base of Eqs.(6-8) of the ^{45}Sc NMR line shape for $\mathbf{B}\|[001]$ are presented by solid line in Fig. 4(a) and (b). Figure 4(a) shows the line shape for the case of EFG with largest principal axis points in $\langle 001 \rangle$ directions only. The contribution from ordered regions, where $\nu_Q = 0$ was included also. The best fit has been achieved for $\mid \nu_Q^0 \mid = 755$ kHz and $\Delta = 210$ kHz. The contribution of homogeneous broadening was estimated as $\delta = 2$ kHz. One can see that calculated NMR line has a strongly asymmetrical shape, which fits very good the right ″shoulder″ of the measured spectrum. The fitting of left ″shoulder″ is not so good. This can be expected because for $\langle 001 \rangle$ orientation of EFG only a positive quadrupole shift of resonance frequency exists (see Eq.(4) when $\theta = 90^0; 0^0$). Therefore, to fit the left shoulder of the observed spectrum the other orientations of EFG axes are required. The negative shift is possible for EFG axes pointing along $\langle 011 \rangle$ and $\langle 111 \rangle$ directions. The reason for this type local distortions can be related to substitutional disorder in the relaxors.

Really, the probability of configurations with k ions of B' type in the nearest neighbourhoods of B' or B'' ions can be written as

$$P_6^k = \frac{6! y^k (1-y)^{6-k}}{k!(6-k)!},\ y = 1/3 \quad (9)$$

One can see that P_6^k for $k = 1, 2, 3$ are close to each other, while the probability of having $k = 6$ or 0 is much smaller than the most probable value $P_m = 0.328$ corresponding to $k = 2$. It is easy to see that configurations with $k = 1, 2, 3$ can be the response of the three afore-mentioned lattice distortions.

Finally, the experimental line shape of ^{45}Sc was well fitted by the following theoretical curve

$$I_q(\nu) = C_0 I_{ord}(\nu) + C_1 I_{<001>}(\nu) + C_2 I_{\langle 110\rangle}(\nu) + C_3 I_{<111>}(\nu) \tag{10}$$

with $C_0 \simeq 0.3, C_1 \simeq 0.45, C_2 \simeq 0.11, C_3 \simeq 0.14$; the subscripts denote the direction of the EFG axes. The result of ^{45}Sc complete spectrum simulation is presented in Fig. 4(b).

The obtained set of fitting parameters (ν_Q and Δ are presented in Table I) permits to describe theoretically the NMR line shapes measured for any other orientation of magnetic field. In particular in Fig. 4(c) and (d) the observed and calculated line shapes for $\mathbf{B}\|[011]$ and $\mathbf{B}\|[111]$ are shown. One can see the good agreement between measured and calculated line shapes.

Similar simulations performed for ^{93}Nb NMR spectra are presented in Fig. 5 and corresponding fitting parameters are listed in Table I. The agreement between measured and calculated spectra seems also good, however, due to small intensity of the wide part of the spectrum obtained parameters may contain significantly bigger miscalculation than that for the ^{45}Sc spectrum.

C. Analysis of ^{93}Nb NMR spectra in PMN

It can be seen from Fig. 3 that practically all the ^{93}Nb spectrum in PMN is strongly broadened in comparison with the dipole-dipole width that is equal to 2.8 - 3.6 kHz (as in the case of PSN). The portion of the spectrum unbroadened by quadrupole mechanism or by anisotropic chemical shift accounts only for 1 - 2 percent of the total intensity. It is clear that the Nb nuclei, which give the contribution into this narrow spectrum, locate at the positions close to the regular cubic ones. Possible origin of these crystal regions will be discussed in the next section.

The wide, main part of the ^{93}Nb spectrum is related to the disordered, locally noncubic, regions of the crystal , as in the case of PSN. Contrary to PSN, the portion of such regions in PMN accounts for 98% of the total volume of the crystal.

^{93}Nb spectrum for disordered PMN was fitted assuming local distortions along <001>, <110> or <111> directions, i.e. as in the case of the PSN by Eq. (8). Because the procedure of the simulation is completely similar to that described for PSN we confined here only presentation in Table I of spectral parameters derived. Compareing spectral data for disordered PSN and PMN one can emphesize a similarity in the symmetry and sometimes even in the values of electric field gradients at Nb positions. One can see also that dispertion in PMN is larger than in PSN. This is in agreement with the fact that in PMN local lattice distortions should be much larger due to bigger difference in the ionic charges of B′ and B″ cations.

Summarizing, three main conclusions should be made.

(i) In the ordered regions, which account up to 30% in the PSN and 2-3% in the PMN of the total crystal volume, lattice ions occupy cubic lattice positions where electric field gradients are close to zero.

(ii) In the disordered regions there are non-zero EFG along pure cubic directions (<001>, <110> or <111>). Because both the PSN and PMN has in average cubic symmetry at T >

T_0, these non-zero EFG can be related to randomly distributed unequal charges of B-type cations and/or random shifts of the ions from their positions in the cubic lattice. In this case the essential part of ions ($\sim$ 30-55%) experiences shift along <001> axes.

(iii) EFG tensor components are significantly distributed around their mean values that manifests in broad asymetric NMR line shape.

D. Numerical calculation of the EFG tensor and NMR line shape

In the previous section on the basis of analytical calculation of the shape of inhomogeneously broadened NMR line the mean values of quadrupole coupling constants in Sc and Nb cation positions as well as their dispertions were obtained. The method applied by us has allowed to take into account only distribution of the quadrupole frequencies (ν_Q), but the presence of random deviations of EFG axes from their most probable directions, i.e the possible fluctuations of $f_\eta(\theta, \varphi)$ (see Eq. (1)) remained discounted. Note that this effect is mainly related to a distant ion contributions. Ignoring of these fluctuations has resulted in too much high values of homogeneous width, which was accordingly 4 kHz and 8 kHz for the ^{45}Sc and ^{93}Nb in PSN and 18 kHz for the ^{93}Nb in PMN. Let′s remind, that dipole width for both the ^{45}Sc and ^{93}Nb accounts only 2.8-3.2 kHz.

The second reason on which we have undertaken numerical calculation of EFG is related to attempt to define ions displacements, which could be responsible for symmetry and magnitude of an EFG in both relaxor systems. Taking into account complexity and substantially uncertainty of local structure of these compaunds we used the simple model of point charge point dipole, which, however, took into account effects related to partial covalency of bonds in the BO_6 octahedron as well as electronic polarizibility of ions. Obviously due to limitations of the point charge model the obtained ions shifts should be considered only as an estimated ones, the degree of which reliability depends on correctness (luck) of a choice of such empirical parameters of ions as their effective charges and polarizibility.

In the point charge point dipole approximation the electric field gradient components at the site of the nucleus are given by

$$V_{ij} = (1 - \gamma_\infty) \sum_k \frac{\partial^2}{\partial x_i \partial x_j} \left[\frac{q_k}{r_k} + \frac{r_{ik}\mu_{ik}}{r_k^3} \right], \tag{11}$$

where q_k and μ_k are the electric point chages and dipole moment on the k-th ion. r_k is the distance between the k-th ion and the observation point, and γ_∞ is the anti-shielding parameter [9]

For the conviencity three contributions into EFG were detached in the whole sum (11). The first contribution ($V_{ij}^{(1)}$) was related to random distribution of charges of B′/B″ ions at lattice points of ideal ABO_3 perovskite structure. Contributions of ions at a distance up to five lattice constants (2 nm) were summed up. However, usually the distance up to 1.2 - 1.5 nm was sufficient due to the rapid decay of V_{ij} with the distance (see Eq. 11). In the calculations the B type ions were randomly distributed at lattice sites with the help of random number generator or they were located in the 1:1 or 1:2 ordered regions. The main condition for any ion configuration was electroneutrality, i. e. the stoichiometric (in average 1:1 for PSN and 1:2 for PMN) composition in the calculated region was conserved.

As an example, the result of the calculation of largest component V_{zz} as a function of polar angle θ for the PMN is presented in Fig. 6. Here we took effective valence charges of Mg^{2+} and Nb^{5+} as one haft of their formal charges. It is seen that V_{zz} lies close or along cubic directions, but it is strongly distributed in both the magnitude and orientation. The mean value $\mid \overline{V_{zz}} \mid = 0.78 * 10^{16}$ V/cm^2 ($\frac{e^2qQ}{h} \simeq 15MHz$) is much less than that expected from coupling constant measured. Thus, this contribution to the EFG can not be responsible for wide component of the ^{93}Nb NMR line. It can give only some contribution to homogenious broadening of NMR line because it leads to distribution of axes directions of the total EFG. Note that in $PbSc_{1/2}Nb_{1/2}O_3$ this part of EFG is neglectly small in comparison even with the dipole-dipole width, that is in good agreement with smaller difference between charges of Sc^{3+} and Nb^{5+} and, in addition, 1:1 type relaxors have more symmetrical distribution of B′/B″ ions.

The second contribution ($V_{ij}^{(2)}$) into EFG took account for the shifts of B′/B″ ions themselves relatively to the nearest six oxygen ions. Possible shifts of Pb^{2+} ions were not taken into account due to their smaller (10-15 times) contribution into EFG for the same values of the shifts.

In a general case for arbitrary B type ion shift with respect to the center of the undistorted oxygen octahedron, the following expressions for EFG tensor components were obtained :

$$
\begin{aligned}
V_{ij}^{(2)} &= -\frac{42 \cdot z_O^{val}}{b^5} d_i d_j, \ i \neq j \\
V_{xx}^{(2)} &= \frac{21 \cdot z_O^{val}}{b^5} (2d_x^2 - d_z^2 - d_y^2) \\
V_{yy}^{(2)} &= \frac{21 \cdot z_O^{val}}{b^5} (2d_y^2 - d_z^2 - d_x^2) \\
V_{zz}^{(2)} &= \frac{21 \cdot z_O^{val}}{b^5} (2d_z^2 - d_x^2 - d_y^2),
\end{aligned}
\tag{12}
$$

where (d_x, d_y, d_z) are vector components of the Nb or Sc shift, z_O^{val} is the effective valence charge of the oxygen, $b = a/2$ (a is the lattice constant). For the simplisity the z_O^{val} was taken as an avarage value over all six oxygen ions. Its value may lay in the range between $-1.63 \mid e \mid$ ($BaTiO_3$ [10]) and $-0.85 \mid e \mid$ ($KNbO_3$ [11]).

The last term in Eq. (11) is related to the induced electric dipole moments μ_i. Assuming that only electronic polarization of the nearest six oxygens gives marked contribution to the EFG (the other ions in the unit cell and the next nearest oxygens give contributions that are an order of magnitude smaller), the dipole contibution is:

$$
\begin{aligned}
V_{xx} &= V_{yy} = -\frac{42\mu}{b^5} d \\
V_{zz} &= \frac{84\mu}{b^5} d,
\end{aligned}
\tag{13}
$$

where μ is assumed to be in the direction of the Z axis of the field gradient.

In the case of <110> and <111> symmetry of lattice distortions nondiagonal components of the EFG tensor have to be also appeared. They are given by expression

$$
V_{ij} = -\frac{84\mu_i}{b^5} d_j, \ i \neq j. \tag{14}
$$

Electronic dipole moment dependes on ionic polarizability and value and direction of ions shifts and it can be usually calculated using knowledge of the polarization and internal electric field. Obviously for disordered relaxors such a way is not suitable because here is only local polarization and large uncertainty in the ions positions. Therefore, for the estimation of V_{ij} we applied a method of effective dipole moments. In particular, it is known, that in perovskite ferroelectrics the spontaneous polarization can be well described by the Born effective charges:

$$P = \frac{\mid e \mid}{\Omega} \sum_s Z_s^* d_s, \tag{15}$$

where Ω is the cell volume, and the Born effective charges Z^* are 0.82(K), 9.13(Nb), -6.58(O_1), -1.68(O_2) in tetragonal phase of $KNbO_3$ [12] and 3.87(Pb), 7.07(Ti), -5.71(O_1), -2.51(O_2) in $PbTiO_3$ [13]. The high values Z^* indicate on larger contribution of electronic dipole part to whole polarization in the comparison with rigid ionic part, that should be as a rule in high polarizable perovskite ferroelectrics [14].

Taking into account a special role of Pb ions, namely their strong hybridization with oxygen ions, we used in our calculations the effective charges derived in $PbTiO_3$. For simplisity the same avaraged value of $Z_O^* = -4 \mid e \mid$ was taken for evaluation of the electronic dipole moment $\mu_i = Z_O^* * d_i$ in expressions (13-14). One can easy see, that under these conditions expressions (12) and (13-14) become similar, thus in the calculation of the whole dipole contribution to the EFG one can use only its electronic part, because $Z_O^* >> Z_O^{val}$. Note that similar results were obtained in $KNbO_3$ [15] and $BaTiO_3$ [16].

Taking into account that the ion shifts can have random values due to the disorder of the Mg, Nb and Sc positions, the ion shift distribution function was assumed in the Gaussian form:

$$f(d) = \frac{1}{\sigma(2\pi)^{1/2}} \exp\left(-\frac{(d-d_0)^2}{2\sigma^2}\right), \tag{16}$$

where d_0 is mean value of the shift and σ is its dispersion.

Complete NMR line shape was calculated taking into account electric-field-gradient contribution, magnetic dipole-dipole interaction, as well as chemical shift mechanisms. Since the contribution of the last mechanism was much less with respect to the quadrupole one it manifests itself only in the central narrow part of the spectrum. Its contribution was accounted by the renormalization of dipole-dipole linewidth. NMR spectrum intensity $I(\nu)$ was obtained by summarizing the contributions of the NMR lines from a large number of clusters in which the B type ions could be shifted in one of three directions: <001>, <011>, <111> with their resonance frequencies given by Eq. (1).

$$I(\nu) = \sum_{n=1}^{N} \exp\left[\frac{(-\ln 2)\cdot(\nu_n - \nu)^2}{\delta^2}\right]. \tag{17}$$

Here, ν_n is the resonance frequency for nucleus in the center of n-th cluster, δ is a half of the dipole-dipole width and N is the total number of clusters (usually, N = 15000 - 20000).

In the calculation of second-order quadrupole shifts for ^{93}Nb the parameter $\gamma_\infty = -16$ was taken as in other ABO_3 crystals like $KNbO_3$ and $LiNbO_3$ [15,17]. For the ^{45}Sc ion the

antishielding parameter is rather uncertain. However, clearly its value has to be smaller of about two times in comparison with ^{93}Nb due to smaller number of electronic orbitals. Value $\gamma_\infty = -9$ leads to the best agreement with the experimental spectrum.

As an example, the results of ^{45}Sc complete spectrum calculation in PSN for several crystal orientations are presented in Fig. 7 and corresponding values of ion shifts as well as their dispersion in Table II. It is seen excelent agreement between measured and calculated spectra including frequency region around ν_L, where analytical method gave much worth fit.

The results of calculation in PMN for two crystal-orientations (B II [001] and [011]) are presented in Fig. 8. The individual contributions which were related to the Nb shifts in different directions with respect to oxygen positions are presented as well. The values of ion shifts and their dispersion obtained by fitting of the experimental NMR spectra are listed in the Table III. Excellent similarity of ion shifts in PMN and disordered PSN is obtained. On the other hand, a large relative dispersion of niobium (or rather oxygen) shift is noted along <111> and <011> directions. Such a large fluctuations in ion shifts can show their dynamic character. Actually, we can not expect full motional narrowing of NMR spectrum, since the frequency shift of the -1/2 $\longleftrightarrow$ 1/2 transition depends on the square of EFG. However, this assumption can be supported by measuring and analysis of NMR spectra changes with decreasing temperature. We plan to carry out such analysis in the nearest future. On the other hand, large dispersion of the quantities is characteristic feature of relaxors.

Three main comments should be made.

(i) The values presented in Table II-III are the relative shifts between Nb(Sc) and oxygen ions, i. e., $d_{Nb(Sc)-O}$. Larger contribution into $d_{Nb(Sc)-O}$ values due to oxygen ions shift rather than that of Nb(Sc) ions is expected in accordance with x-ray data [3].

(ii) The real values of ion shifts can be somewhat different from those given in the Tables II-III due to simplifications allowed in the calculations, including point charges model. However the conclusion about existence of the displacements, their directions and dispersion is not related to the model of EFG calculation because it follows directly from observed shape and width of ^{45}Sc and ^{93}Nb NMR lines.

(iii) In the ordered regions the Sc^{3+}, $Nb^{5+}$and O^{2-} ions occupy completely cubic lattice positions, i. e. they are not shifted. On the contrary, in the disordered regions these all ions are randomly shifted away from their cubic lattice sites in one of the directions: <001>, <011>or <111>. The larger part of ions ($\sim$50%) experiences shift along <001>axes.

IV. DISCUSSION

Evidently, basic question in the understanding of the origin of unusual physical properties of relaxor ferroelectrics is their local structure, because at any temperature and even on a micrometric scale the average symmetry is cubic rather than any lower one (see, for instance, [18,19] and references therein). Note, that the existence of diffusive scattering in the powder neutron diffraction patterns observed in PMN below 340 K was interpreted in Ref. [20] as the occurrence of local polar order inside the average paraelectric matrix. However, it is still a matter of debate whether this polar order is organized as small ferroelectric domains or as a dipole glass. In contrast to PMN, PSN at $T < T_C$ ($T_C \approx$ 350-360 K) undergoes into the $R3m$ rhombohedral ferroelectric phase [3,21]. Moreover, this crystal can be easily obtained in 1:1 Sc/Nb ordered state. It is important to emphasise that the polar long range order

appears not only in perfect 1:1 Sc/Nb ordered PSN, but even in compositionally disordered crystal [3], i. e. the compositional disorder does not prevent establishing at least partly of a long-range order . To our mind this may correspond to mixed ferro-glass phase. It is important to compare PSN and PMN local structure on the base of NMR data because many of novel models, which explain the behaviour of PMN at low temperatures, are based on the existence of 1:1 Mg/Nb ordered micro-regions similar to 1:1 Sc/Nb regions in PSN.

It is clearly seen from Figs. 1 and 2 that for 1:1 ordered regions in the PSN distinctive narrow line in both ^{45}Sc and ^{93}Nb NMR spectra are obtained. In these regions Sc and Nb ions are located in regular cubic lattice sites, where the total electric-field-gradient is zero or close to zero. The ^{93}Nb NMR spectrum in PMN also exhibits narrow component (Fig. 3) but its integral intensity is only of about 1.5 - 2 percent of the total spectrum intensity (Tables II,III). Evidently, it is reason to ascribe this ^{93}Nb resonance to the regular 1:2 Mg/Nb ordered regions of the crystal. Note that this resonance could not belong to 1:1 Mg/Nb ordered regions because in agreement with high resolution electron microscopy study [22] the portion of such ordered regions (if they exists) should be approximately 30%. Thus, if local ($\sim$ 1.5 - 2.5 nm) 1:1 ordered clusters exist in PMN, the disagreement between NMR and electron microscopy data can be overcame in supposition that in these local regions niobium and oxygen ions are shifted as in completely disordered regions. This fact seems to be strange. Let us remind that in 1:1 Sc/Nb ordered PSN the Sc and Nb ions are situated in correct cubic lattice sites. Taking into account this argument, the model grounded on the alternation of Nb and ($Mg_{2/3}Nb_{1/3}$) layers which also explains the observation of 1/2 <111> superlattice diffraction peak [23,24] seems to be more convincing. In this model local strains induced by the charge disbalance between the Nb and Mg/Nb layers can be locally compensated by oxygen ion displacements which will give the contribution in the electric field gradient. Additional contribution to EFG is also due to ($Mg_{2/3}Nb_{1/3}$) layer compositional disorder.

Obtained evidence about three possible directions of Nb ions shift relatively the surrounding ions (so that oxygen and lead ions shift can contribute also) seems to be very important. Physical nature of this phenomenon can be related to substitutional disorder in the relaxors $A(B'_{1/3}B''_{2/3})O_3$.

We can not exclude also that ion shift in one out of three observed directions may be the result of ferroelectric phase transition which could be at Burns temperature $T_d = 640$ K [25]. However with the temperature decrease strong random fields completely destroy this ferroelectric long range order because of correlation radius r_c decrease at $T < T_d$ (here r_c is the correlation radius of the lattice that should be responsible for the phase transition at T_d) [26]. As a result only a small movable polar clusters appear below T_d. In such a picture strong dispersion and V-F law, observed in the temperature dependence of dielectric permitivity in PMN (see, e.g. [27] and ref. therein) can be considered as manifestation of reentrant phase (like that in magnetic systems [28]) of aforementioned Burns reference phase.

To clear up all aforementioned questions precise measurements of NMR spectra in the vicinity of the Burns temperature are extremely desirable.

Finally, we would like to point out that proposed methods of NMR line shape analysis can be applied to other disordered materials where the NMR frequency shift is a nonlinear function of the random electric field gradients.

REFERENCES

[1] G. A. Smolenskii and V. A. Isupov, Dokl. Akad. Nauk SSSR **97**, 653 (1954).
[2] L. E. Cross, Ferroelectrics **76**, 241 (1987).
[3] C. Malibert, B. Dkhil, J. M. Kiat, D. Durand, J. F. Berar, and A. Spasojevic-de Bire, J. Phys.: Condens. Matter, **9**, 7485 (1997).
[4] M. D. Glinchuk, V. V. Laguta, I. P. Bykov, S. Nokhrin, V. P. Bovtun, M. A. Leschenko, J. Rosa, and L. Jastrabik, J. Appl. Phys. **81**, 3561 (1997).
[5] R. Blinc, J. Dolinšek, A. Gregorovič, B. Zalar, C. Filipič, Z. Kutnjak, A. Levstik, and R. Pirc, Phys. Rev. Lett. **83**, 424 (1999).
[6] R. Blinc, A. A. Gregorovič, B. Zalar, R. Pirc, V. V. Laguta, and M. D. Glinchuk, J. Appl. Phys. **89**, 1349 (2001).
[7] A. Abragam, *The Principles of Nuclear Magnetism* (Clarendon, Oxford, 1961).
[8] M.D. Glinchuk, I.V. Kondakova, Sov. Sol. St. Phys., **40**, 340 (1998).
[9] T. P. Das, R. Bersohn, Phys. Rev., **102**, 733 (1956).
[10] R. E. Cohen, H. Krakauer, Phys. Rev. **B42**, 6416 (1990).
[11] R. I. Eglitis, A. V. Postnikov, and G. Borstel, Phys. Rev. **B54**, 2421 (1996).
[12] R. Resta, M. Posternak, and A. Baldereschi, Phys. Rev. Let. **70**, 1010 (1993).
[13] U. V. Waghmare and K. M. Rabe, Phys. Rev. **B55**, 6161 (1997).
[14] W. Zhong, R. D. King-Smith, and D. Vanderbilt, Phys. Rev. Lett., **72**, 3618 (1994).
[15] R. R. Hewitt, Phys. Rev., **121**, 45 (1961).
[16] A. S. Viskov and Yu. N. Venevcev, Fiz. Tverd. Tela (in Russian), **8**, 416 (1966).
[17] G. E. Peterson and P. M. Bridenbaugh, J. of Chemical Physics, **43**, 3402 (1968).
[18] P. Bonneau, P. Garnier, G. Calvarin, E. Husson, J. R. Gavarri, A. W. Hewat, and A. Morell, Journal of Solid State Chemistry, **91**, 350 (1991).
[19] N. -de Mathan, E. Husson, G. Calvarin, J. R. Gavarri, A. W. Hewat, and A. Morell, J. Phys.: Condens. Matter, **3**, 8159 (1991).
[20] de Mathan, E. Husson, and A. Morell, Mater. Res. Bull., **27**, 867 (1992).
[21] K. S. Knight and K. Z. Baba-Kishi, Ferroelectrics, **173**, 341 (1995).
[22] C. Boulesteix, F. Varnier, A. Llebaria, and E. Husson, J. of Solid State Chemistry, **108**, 141 (1994).
[23] T. Egami, W. Dmowski, S. Teslic, P. K. Davies, I. -W. Chen, and H. Chen, Ferroelectrics, **206-207**, 231 (1998).
[24] J. Chen, H. M. Chan, and M. P. Harmer, J. Amer. Cer. Soc.,**72**, 593 (1989).
[25] G. Burns and F. H. Dacol, Phys. Rev. B, **28**, 2527 (1988).
[26] M. D. Glinchuk and R. Farhi, J. Phys.: Condens. Matter, **8**, 6985 (1996).
[27] M. D. Glinchuk and V. A. Stephanovich, J. Appl. Phys., **85**, 1722 (1999).
[28] J. Ya. Korenblit and E. F. Shender, Usp. Fiz. Nauk, **157**, 267 (1989).

TABLES

TABLE I. ^{45}Sc and ^{93}Nb quadrupole coupling constants and their dispertion measured in disordered PSN and PMN at T = 450 K.

Compound	$\frac{e^2qQ}{h}$ (MHz)	Δ (MHz)	$\mid V_{zz} \mid$ ($10^{20} Vm^{-2}$)	Orientation of V_{zz}
$PbMg_{1/3}Nb_{2/3}O_3$				
^{45}Sc	10.6	2.9	20	<001>
	9.1	4.9	17	<011>
	8.8	4.9	16	<111>
^{93}Nb	46	15	68	<001>
	42	20	62	<011>
	56	27	83	<111>
$PbMg_{1/3}Nb_{2/3}O_3$				
^{93}Nb	46	24	68	<001>
	60	29	89	<011>
	36	29	53	<111>

TABLE II. Parameters of ions shifts in PSN at T = 420 K derived from NMR data.

		direction of ions shifts		
	1:1 ordered	<001>	<011>	<111>
portion (%)	30	35	15	18
d_{Sc-O} (nm)	0	0.015	0.016	0.017
σ (nm)	0	0.001	0.001	0.001
d_{Nb-O} (nm)	0	0.016	0.018	0.022
σ (nm)	0	0.005	0.005	0.005

TABLE III. Parameters of ions shifts in PMN at T = 450 K derived from NMR data.

		direction of ions shifts		
	1:2 ordered	<001>	<011>	<111>
portion (%)	2	56	21	21
d_{Nb-O} (nm)	0	0.016	0.021	0.017
σ (nm)	0	0.005	0.01	0.01

FIGURES

FIG. 1. ^{45}Sc NMR spectra in PSN. The diagrams schematecally show expected NMR resonances for second order quadrupole contribution with EFG axis pointed at $< 001 >$ directions.

FIG. 2. ^{93}Nb NMR spectra in PSN. The inset shows the ^{93}Nb spectrum measured by sweep of the irradiation frequency.

FIG. 3. ^{93}Nb NMR spectra in PMN.

FIG. 4. Comparison between experimental (points) and calculated (solid line) ^{45}Sc NMR line shapes in PSN for a) and b) $\mathbf{B}\|[001]$; c) $\mathbf{B}\|[011]$; d) $\mathbf{B}\|[111]$. Calculated line shapes include contribution from ideal structure regions plus axial EFG pointed at a) $\langle 001 \rangle$ directions; b), c) and d) $\langle 001 \rangle$, $\langle 011 \rangle$, $\langle 111 \rangle$ directions.

FIG. 5. Comparison between experimental (points) and calculated (solid line) ^{93}Nb NMR line shapes in PSN for a) $\mathbf{B}\|[001]$; b) $\mathbf{B}\|[011]$.

FIG. 6. Polar plot of the $\mid V_{zz} \mid$ EFG component at Nb sites in PMN calculated for Mg^{2+} and Nb^{5+} random distribution at lattice points of ideal ABO_3 structure.

FIG. 7. Measured and calculated ^{45}Sc NMR spectra in PSN at orientation (a) B II [001] and (b) B II [011]. Separated contributions into NMR spectrum connected with different type of ion shifts are shown in the bottom panels by: solid line (d_{Sc-O} II <001>), dash line (d_{Sc-O} II <011>) and dot line (d_{Sc-O} II <111>); contribution from 1:1 Sc/Nb ordered regions is shown by dash dot line.

FIG. 8. Measured and calculated ^{93}Nb NMR spectra in PMN at orientation (a) B II [001] and (b) B II [011]. Separated contributions into NMR spectrum connected with different type of ion shifts are shown in the bottom panels by: solid line (d_{Nb-O} II <001>), dash line (d_{Nb-O} II <011>) and dot line (d_{Nb-O} II <111>); contribution from 1:2 Mg/Nb ordered regions is shown by dash dot line.

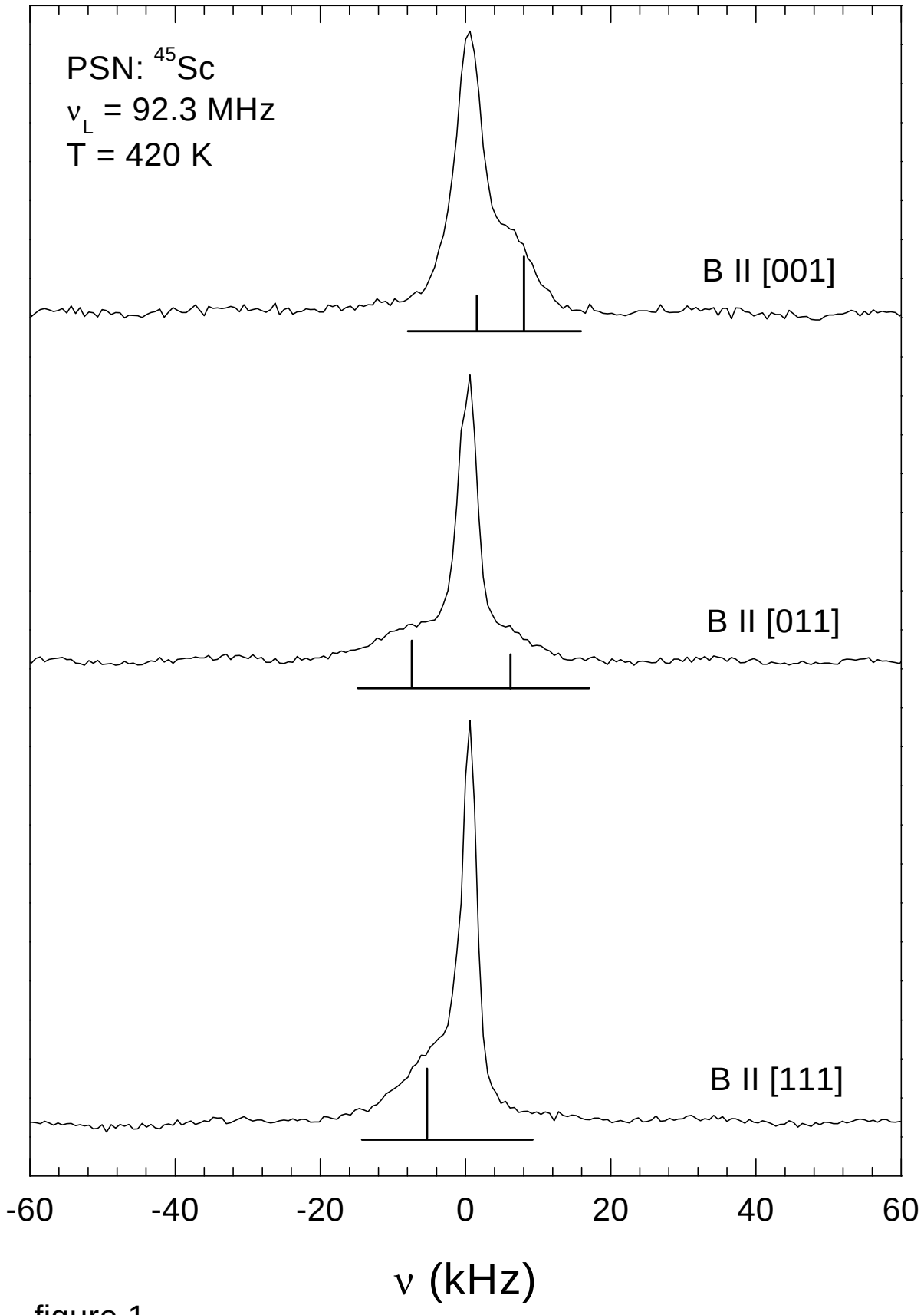
PSN: 45Sc
νL = 92.3 MHz
T = 420 K
B II [001]
B II [011]
B II [111]
-60
-40
-20
0
20
40
60
ν (kHz)

figure 1

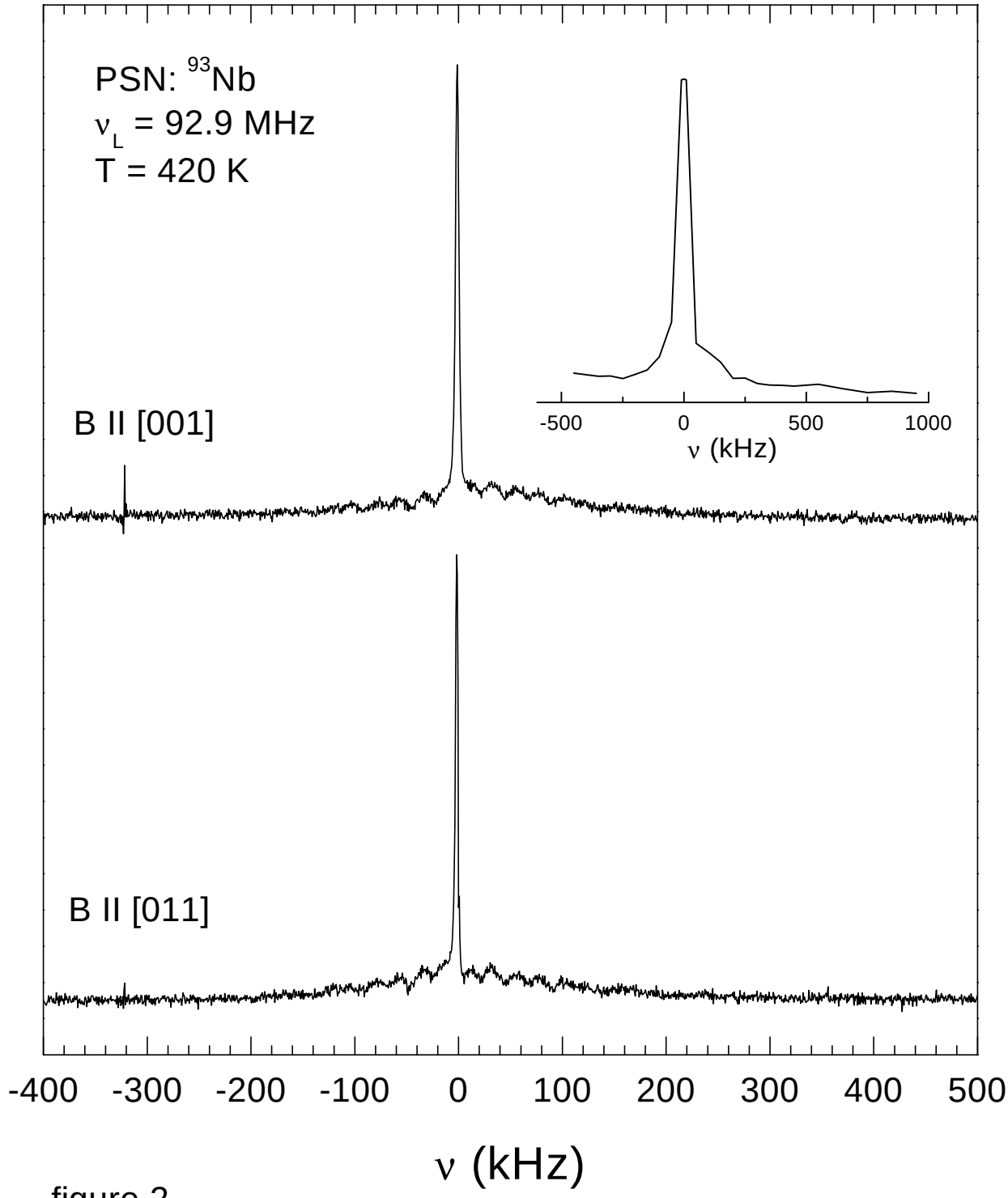
PSN: ^{93}Nb
ν_L = 92.9 MHz
T = 420 K
B II [001]
B II [011]
-500
0
500
1000
ν (kHz)
-400
-300
-200
-100
0
100
200
300
400
500
ν (kHz)

figure 2

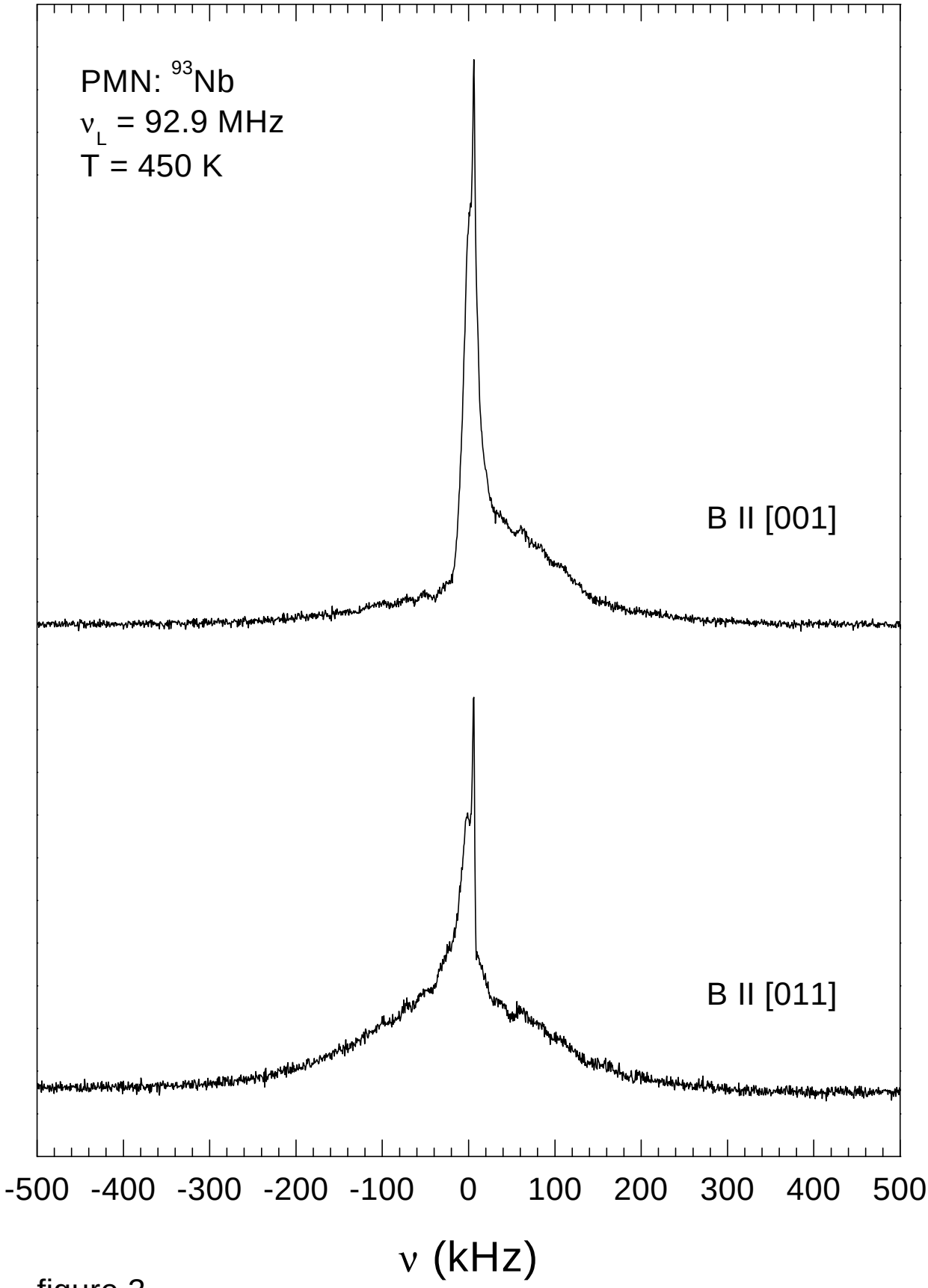
PMN: ^{93}Nb
ν_L = 92.9 MHz
T = 450 K
B II [001]
B II [011]
-500 -400 -300 -200 -100 0 100 200 300 400 500
ν (kHz)

figure 3

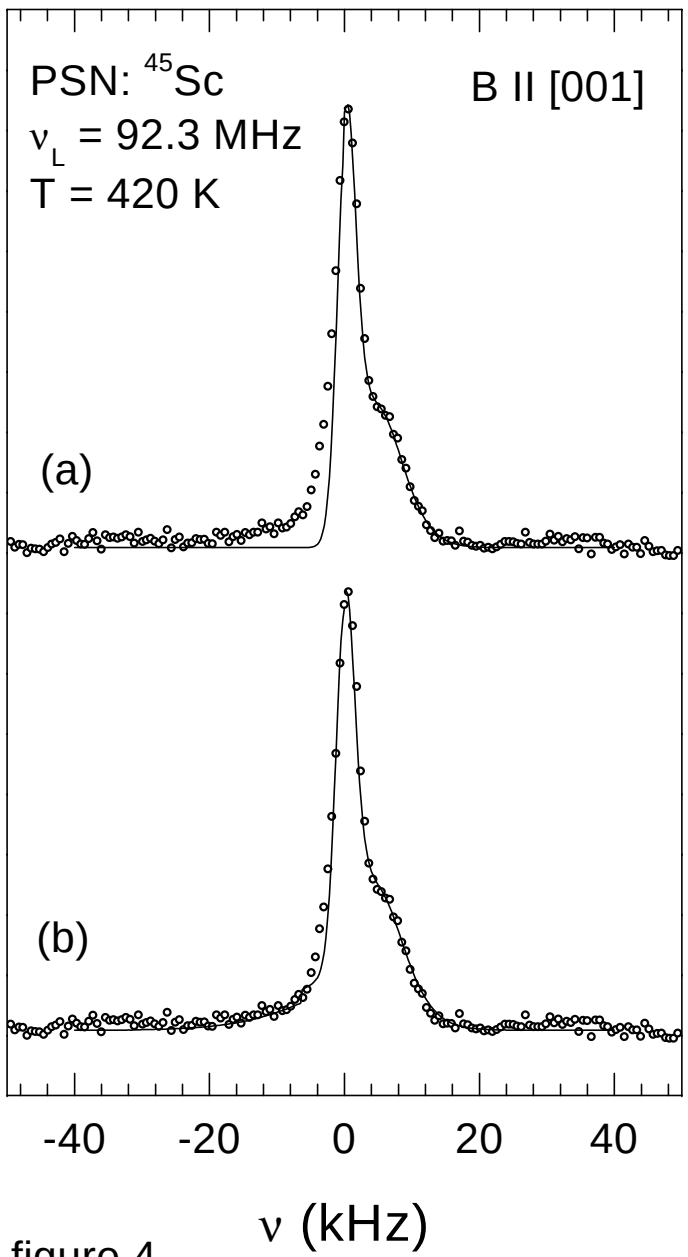
PSN: 45Sc
B II [001]
νL = 92.3 MHz
T = 420 K
(a)
(b)
-40
-20
0
20
40
ν (kHz)

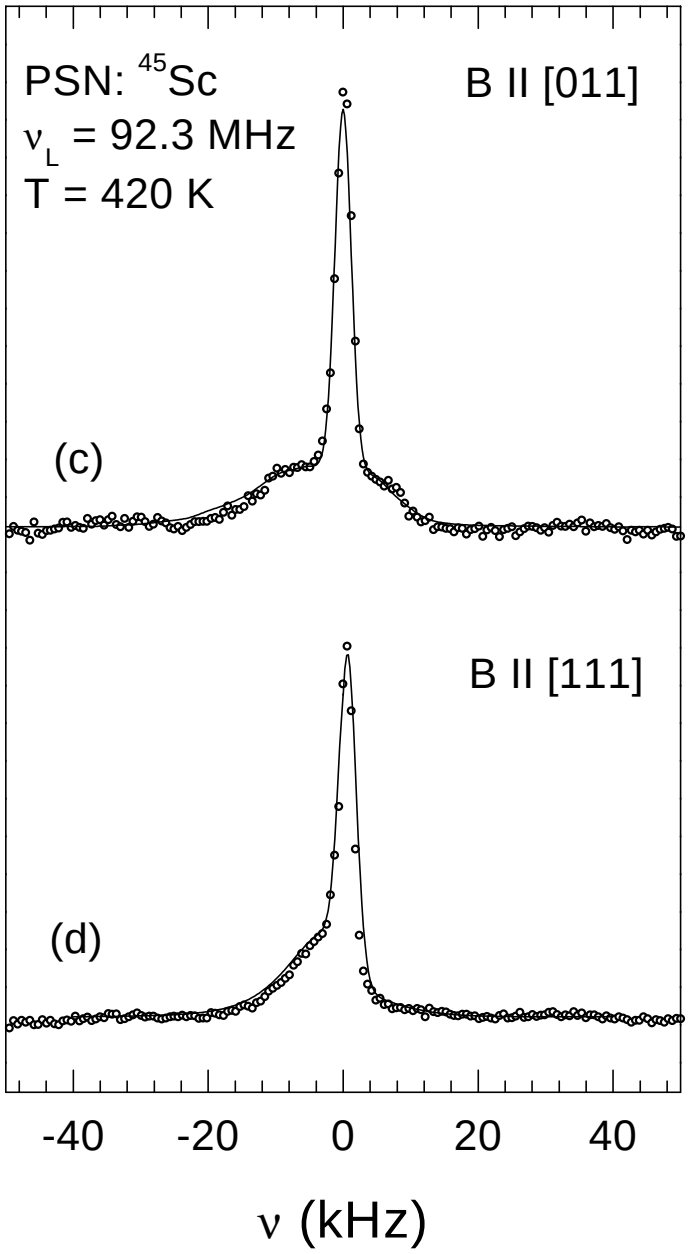
PSN: 45Sc
B II [011]
νL = 92.3 MHz
T = 420 K
(c)
B II [111]
(d)
-40
-20
0
20
40
ν (kHz)

figure 4

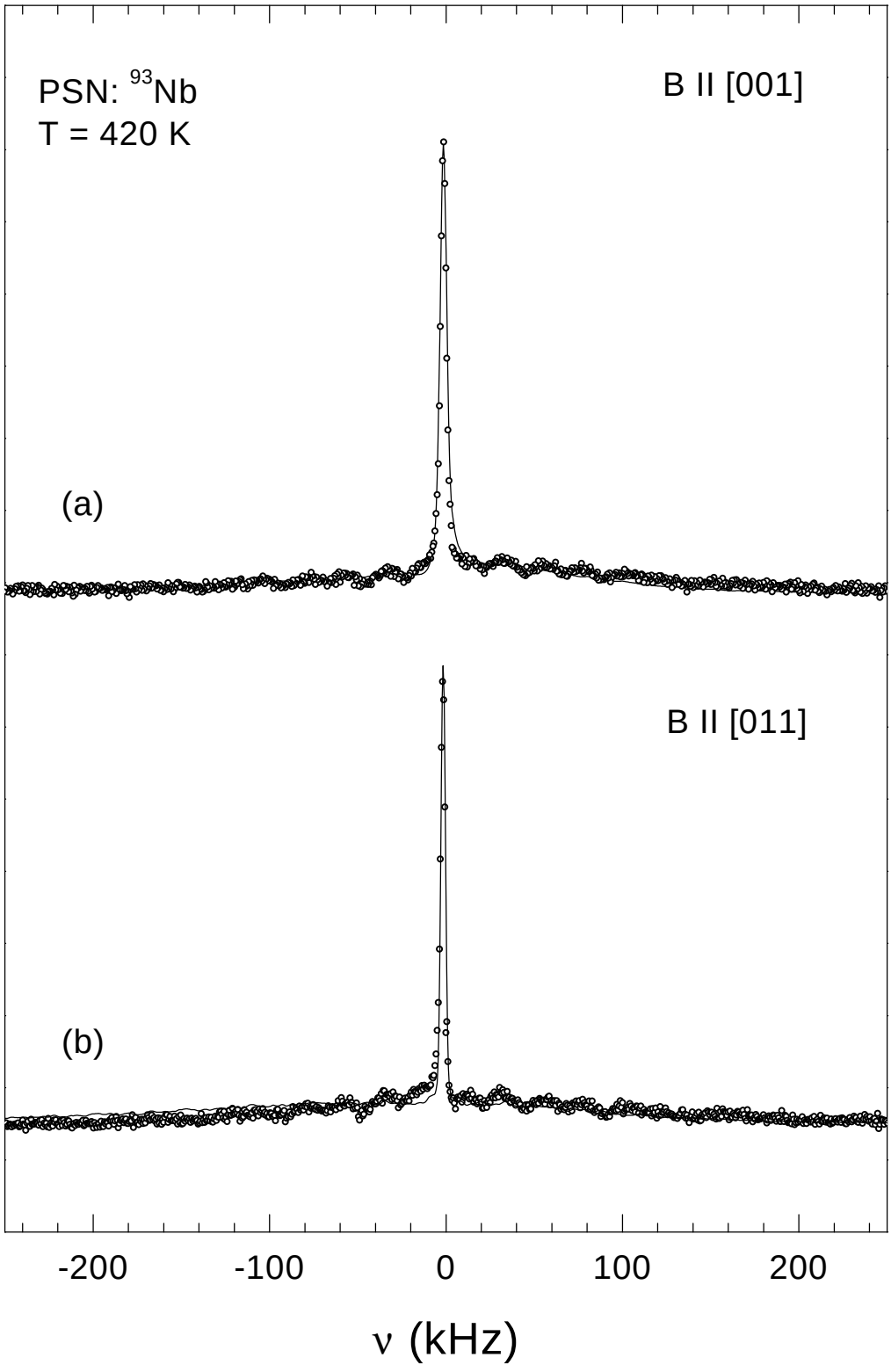

figure 5

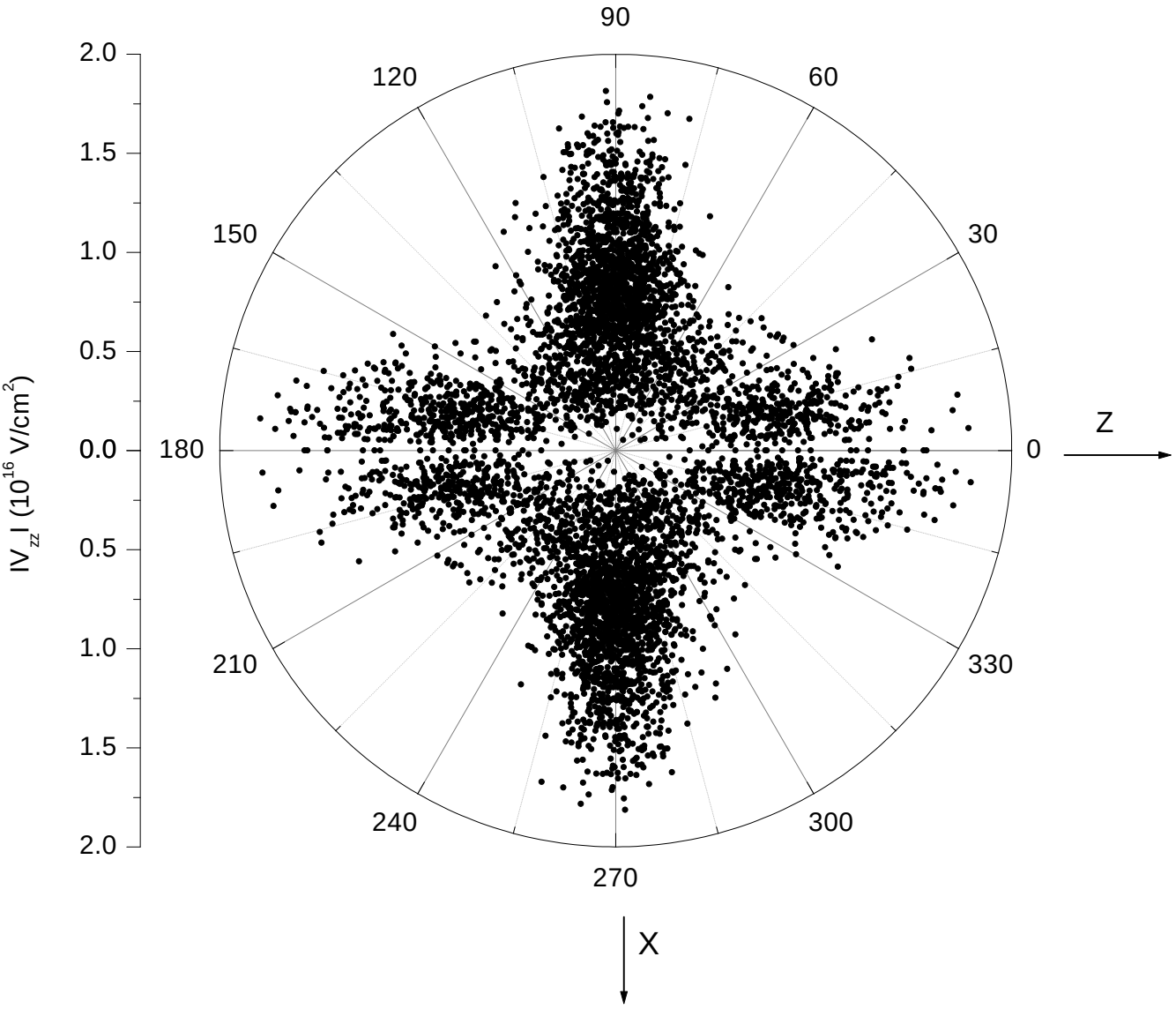
90
120
60
150
30
180
0
210
330
240
300
270
Z
X
2.0
1.5
1.0
0.5
0.0
0.5
1.0
1.5
2.0
$|V_{zz}|$ (10^{16} V/cm^2)

figure 6

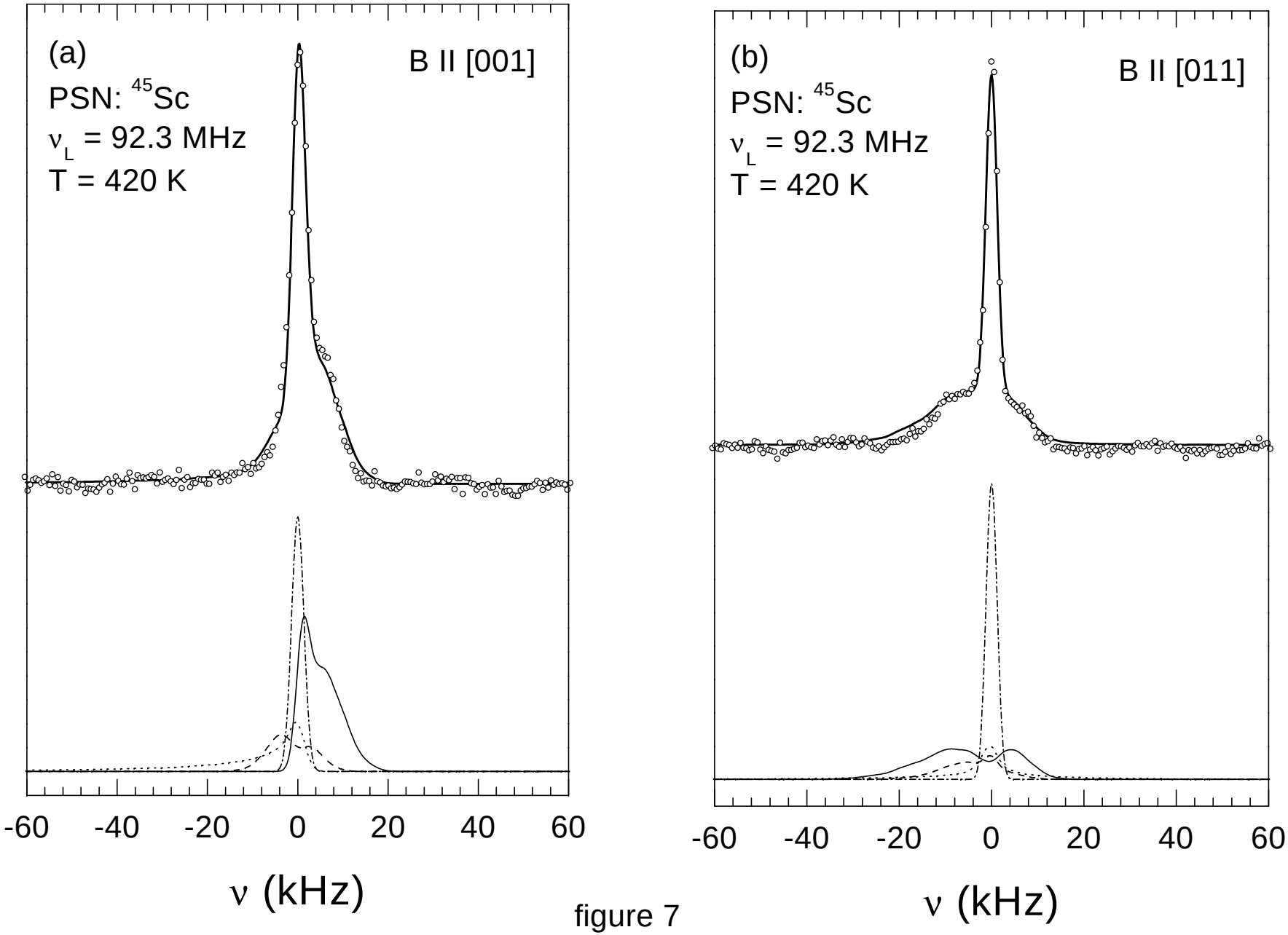
(a)
PSN: 45Sc
νL = 92.3 MHz
T = 420 K
B II [001]
(b)
PSN: 45Sc
νL = 92.3 MHz
T = 420 K
B II [011]
-60
-40
-20
0
20
40
60
ν (kHz)
-60
-40
-20
0
20
40
60
ν (kHz)

figure 7

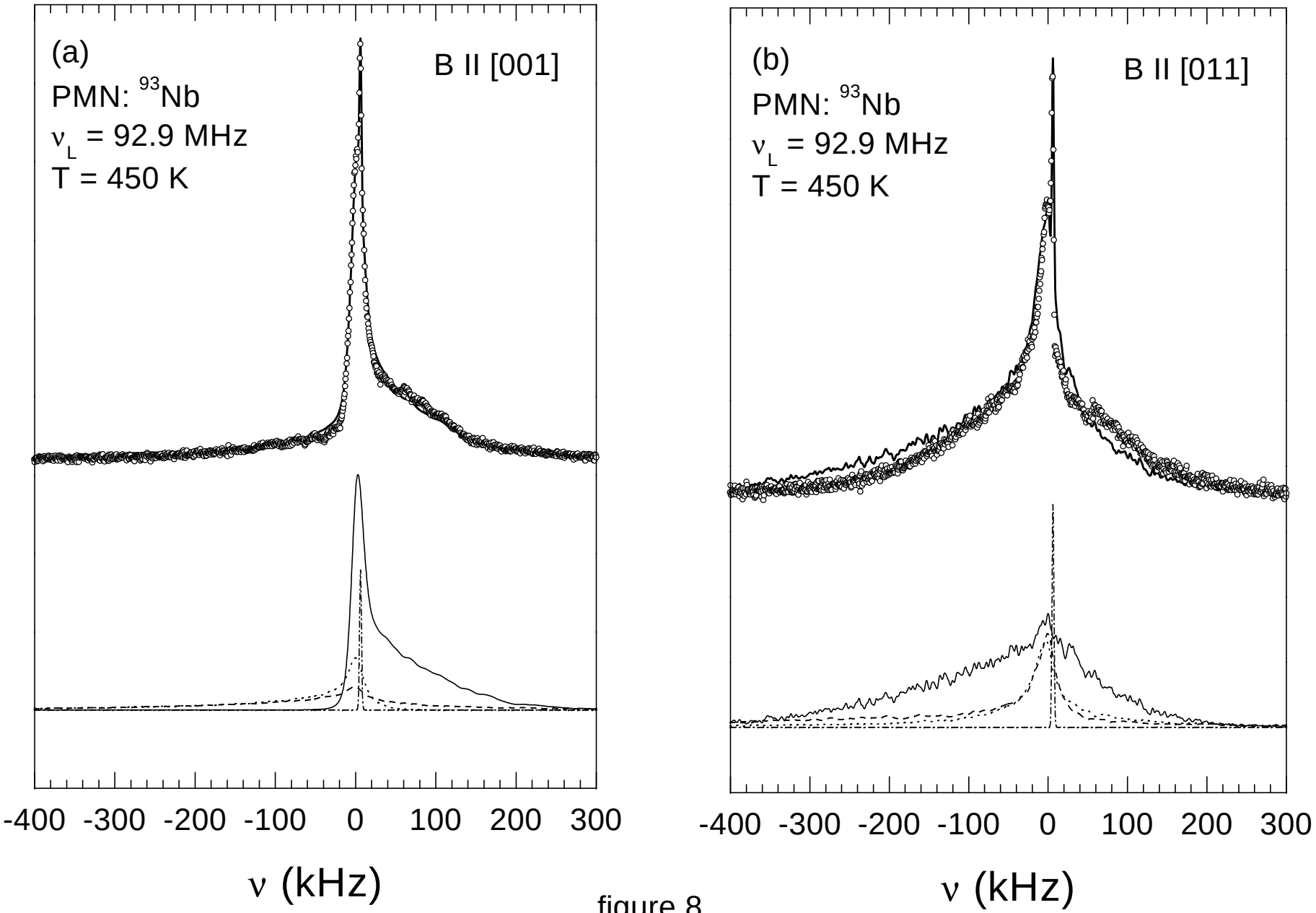
(a)
PMN: ^{93}Nb
ν_L = 92.9 MHz
T = 450 K
B II [001]
(b)
PMN: ^{93}Nb
ν_L = 92.9 MHz
T = 450 K
B II [011]
-400 -300 -200 -100 0 100 200 300
-400 -300 -200 -100 0 100 200 300
ν (kHz)
ν (kHz)

figure 8